Functional Electrical Stimulation of the Latissimus Dorsi Muscle for Use in Cardiac Assist

ADEL M. MALEK AND ROGER G. MARK, MEMBER, IEEE

Abstract—**Direct and nondirect nerve stimulation modes of the thoraco-dorsal nerve (TDN) leading to the latissimus dorsi muscle (LDM) were evaluated by using nerve cuff electrodes (NCE) and intramuscular electrodes (IME), respectively. Following electrode implantation, the LDM was chronically stimulated for two months to induce muscle transformation to oxidative, fatigue-resistant type I muscle fibers. Threshold and impedance values were measured regularly to establish the stability of the implants. The LDM was then dissected, shaped into a ventricle, subjected to a hydraulic load and stimulated using a controlled-voltage pulse-train stimulator with adjustable parameters. Electrical input and hydraulic output variables were measured to obtain the recruitment characteristics and to compare the efficiency of the two types of electrodes.**

Results indicate a tradeoff between the NCE's lower threshold, higher recruitment, and lower energy consumption at saturation, and the IME's greater mechanical stability and better long-term reproducibility.

INTRODUCTION

THERE has recently been an increasing effort in using autologous skeletal muscle pedicles of latissimus dorsi muscle (LDM) to provide power to the failing heart. Synchronously-paced LDM has been wrapped around the heart by Carpentier [4] and Magovern [14] to increase the effective cardiac contractility of patients having impaired or missing left ventricles. In addition to these dynamic cardiomyoplasty operations, research by Stephenson [1]–[3], Chiu [5], [6], [17], and others has centered around using the LDM pedicle as a contracting pouch connected to the descending aorta. Although previous work by Kantrowitz [10], [11] was discouraging because of early muscle fatigue, advances in muscle transformation to type I oxidative and fatigue-resistant fibers [13], [19] have renewed interest in the field.

Once the transformed LDM is formed into a pouch, it can be paced during diastole to operate as an extra-aortic balloon (EABP) diastolic counterpulsator in a fashion similar to the intra-aortic balloon pump (IABP) [18] that is successfully used today in coronary care units. The contraction of such an LDM-powered EABP during diastole would increase the mean diastolic aortic pressure with a resulting increase in coronary and peripheral perfusion and a subsequent lower end-diastolic aortic pressure or afterload: such a mode of operation requires that the LDM provide 10–20 percent of the output of a healthy left ventricle. The goal is to decrease the pressure work on the heart and therefore oxygen demand while increasing its oxygen supply.

A muscle-powered EABP would be of interest in patients having chronic ischemic heart disease or cardiomyopathy accompanied by chronic heart failure, who do not meet cardiac transplantation criteria. It is also intended to be a completely implantable solution whereby the balloon and the LDM would be inserted in the thoracic cavity and the muscle paced by a special-purpose implantable stimulator. This paper is concerned with the functional electrical stimulation of the LDM for use in such an application.

As the techniques of using LDM and other skeletal muscle such as pectoralis major, rectus abdominis, or diaphragm muscle become improved, selecting a proper electrode stimulation mode that is effective, efficient, and stable becomes critical. Two experimental types of electrodes are evaluated in the present study: first, a bipolar nerve cuff electrode (NCE), Medtronic Model SP4080, for direct stimulation of the thoraco-dorsal nerve leading to the LDM; second, an intramuscular electrode (IME) placed in the LDM near the TDN branching consisting of electrode Models SP5528 and SP5537 [8].

MATERIALS AND METHODS

Electrode Implantation

Five mongrel dogs (22–27 kg) were anesthetized with 4 percent Biotal (thyomylal sodium) then kept on a surgical plane using 1.5 percent Halothane. On one side of the subject the SP4080 nerve cuff electrode (Fig. 1) was placed around the TDN 1.5 cm proximal to the branching of the nerve. The intramuscular electrode consisting of the SP5528 (cathode) and SP5537 (anode) was then implanted on the contralateral side: the SP5528 [Fig. 2(a)] was inserted under the three TDN branches in a serpentine manner 1.5 cm distal to the nerve branching point and sutured at both ends; approximately 2 cm of exposed electrode wire was exposed. The SP5537 [Fig. 2(b)] helical screws were inserted 6 cm distal to the SP5528 between the nerve branches (Fig. 3). All electrodes were anchored to surrounding soft tissue to minimize pulling and

Manuscript received June 9, 1988; revised December 13, 1988. This work was supported in part by Medtronic Inc., Cardiac Assist Systems, Minneapolis, MN. The experimental work was conducted at the Physiological Research Laboratories, a division of Medtronic, Inc.

A. M. Malek is with Harvard Medical School, Boston, MA 02115.

R. G. Mark is with Harvard-M.I.T. Division of Health Sciences and Technology, Cambridge, MA 02139.

IEEE Log Number 8927443.

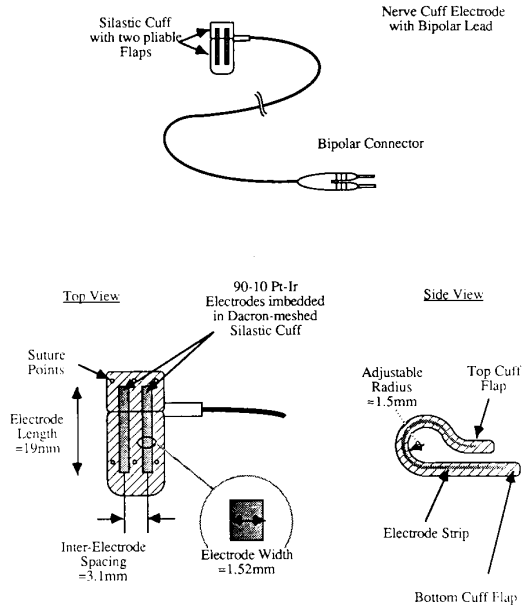

Fig. 1. Nerve cuff electrode (NCE), medtronic model SP4080 showing the overall structure and the various dimensions of interest.

torquing forces. Thin-wire percutaneous extensions were connected to the electrodes and externalized through the dorsum approximately 3–5 cm caudal to the scapulae.

Chronic Stimulation and Muscle Transformation

One week following electrode implantation the NC and IM electrodes were connected to Medtronic Itrel™ voltage-controlled pulse-train generators with zero net area biphasic pulses. The Itrel generators were fastened to the interior of a protective jacket worn by the subjects thus isolating the percutaneous extensions from external forces. The reference output parameters were: pulse width = 230 μs, pulse-train duration = 190 ms, and pulse-train frequency = 36 Hz. The rate of contraction was 15/min for week 2, 30/min for week 3, 45/min for week 4, and 60/min for weeks 5–9 post-implant. The stimulation voltage amplitude was approximately 2–3 times threshold.

Threshold and Impedance Evaluation

Threshold stimulation was obtained by visually identifying the onset of LDM contraction under controlled lighting conditions and body positioning. Voltage and current across and into the electrodes were measured using a Metrabyte DAS16-F high-speed A/D board on a IBM PC-AT microcomputer with a 50 kHz sampling rate/channel. Single pulse studies were carried at regular intervals following implant to determine the strength-duration characteristics of each electrode. The rheobase and chronaxie were derived by using a least-squares fit of Lapicque's equation [12] through the data points corresponding to ten pulse-widths ranging from 50 to 410 μs which were picked in a random order to minimize bias.

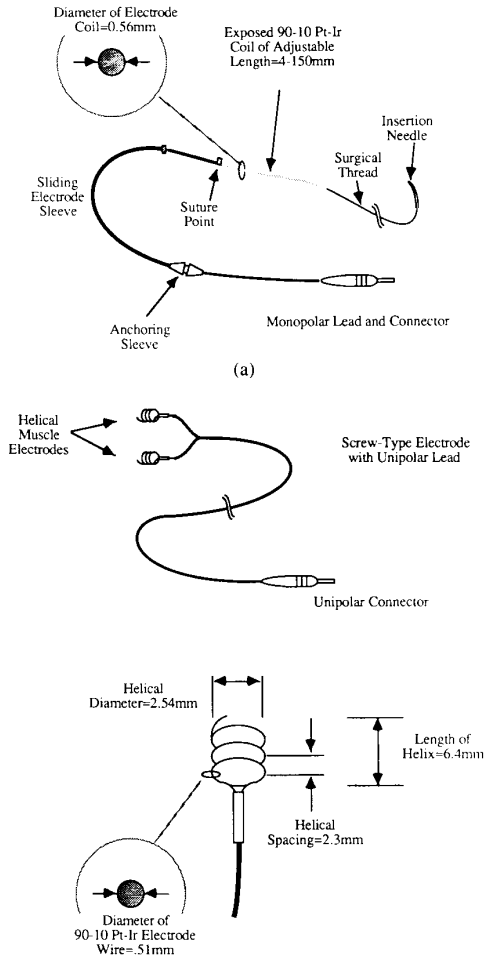

Fig. 2. (a) Intramuscular electrode with adjustable exposed electrode area, medtronic model SP5528. This electrode serves as the cathode in the intramuscular electrode (IME) system. (b) Screw-type intramuscular electrode, medtronic model SP5537. This electrode serves as the anode in the intramuscular electrode (IME) system.

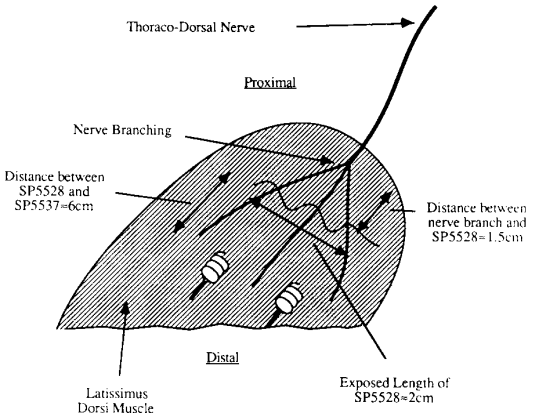

Fig. 3. Placement of the cathode and anode of the intramuscular electrode (IME) system with respect to the thoraco-dorsal nerve and its branches.

Fig. 12 presents a set of this series of ten points taken on different days (fit of Lapicque's equation is not shown) following implant for dog 1.

Typical sampled single pulse voltage stimulus pulse and current response pulse appear in Fig. 4(a) and (b), respectively. From the current waveform one can deduce that the electrode-tissue impedance can be modeled as a resistance (R_1) in series with a parallel RC circuit (R_2 and C) [7]. Although the parameters of such a model circuit could be estimated from the exponential current response waveform to the input voltage pulse, the resulting impedance expression would be frequency-dependent. For the sake of simplicity, the impedance presented here as the resistance index (RI) is an estimate equal to the average of the voltage to current ratio during the stimulus pulse. Considering that the current response to a voltage step is the sum of a step and a dying exponential [Fig. 4(b)], the resistance index is therefore always larger than the entry resistance (R_1) by an amount that is related to the time constant of the impedance. This can be understood by considering the response to a step in voltage: the effective resistance is initially equal to R_1 at the onset of the voltage step (C behaves like short-circuit while charging) and approaches the sum of R_1 and R_2 as time exceeds 4–5 times constants of the circuit (C behaves like an open-circuit when charged).

Evaluation of Muscle Function

Following the two-month muscle transformation and electrode evaluation period the LDM was isolated without affecting its nerve or blood supply, mounted on an oval template, and shaped into a single-layered muscle pouch. A 100 ml latex bladder of paraboloidal shape was then inserted into the muscle pouch and then connected to a hydraulic loading setup (Fig. 5) allowing independent adjustment of preload and afterload. A Statham P23AA pressure transducer was mounted below the afterload tank which is isolated from the bladder at rest by a one-way valve. This allowed the measurement of pressure above the valve and therefore the computation of the afterload pressure at the level of the latex bladder following measurement of the vertical distance between the transducer and the bladder. The water within the loading setup was heated and maintained within 5–10° of 37°C. The pressure inside the bladder was measured with a Statham P23AA pressure transducer while the flow at the opening of the bladder was measured using an In Vivo Metrics FW2-A constant-magnet flowmeter. The voltage and current input to the electrodes were sampled at 50 kHz each, and the pressure inside the latex bladder and the flow in and out of it were sampled at 185 Hz then low-pass filtered using a Blackman LPF with 45 Hz cutoff. Contributions beyond 45 Hz were not considered representative of muscle contraction per se. Typical pressure and flow sampled waveforms during a contraction appear in Fig. 6(a) and (b), respectively. The stimulator parameters were

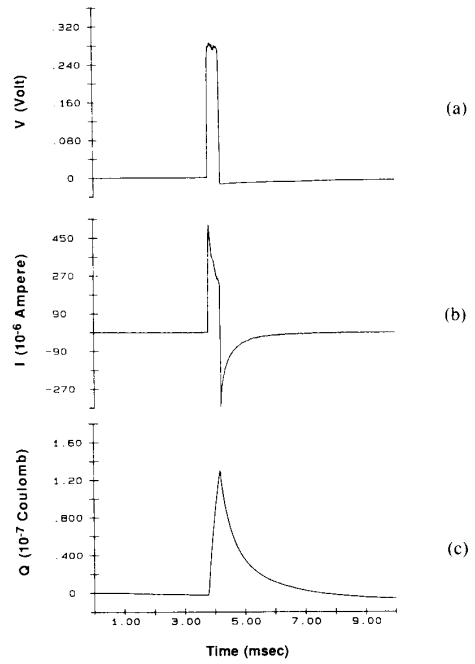

Fig. 4. Typical digitized voltage and current waveforms sampled at 50 kHz using a controlled-voltage source. Charge is obtained by integrating the current waveform with respect to time (from dog 5 NCE, day 73): (a) Voltage, V; (b) Current, I; (c) Displaced charge, Q.

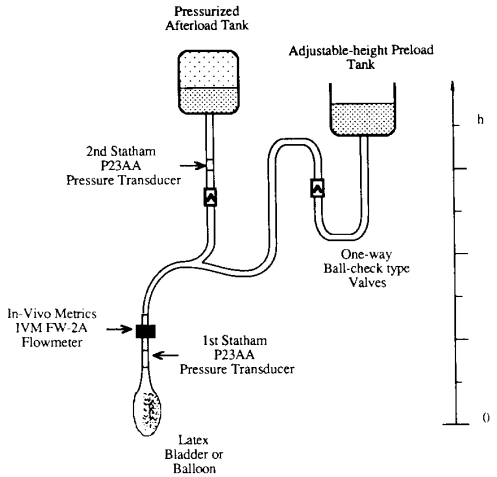

Fig. 5. Schematic diagram of the hydraulic loading setup showing the main functional components. The afterload pressure is adjusted by using compressed air; relief air tanks are connected to the afterload tank to effectively increase its volume and reduce artifactual pressure increases resulting from the fluid displacement into the afterload tank. The preload pressure is adjusted by modifying the height of the preload tank.

adjusted at the reference parameters. Sampling by the computer was initiated immediately after the pulse-train stimulator was triggered by the D/A output channel of the DAS16-F card. Thus both the electrical input and hy-

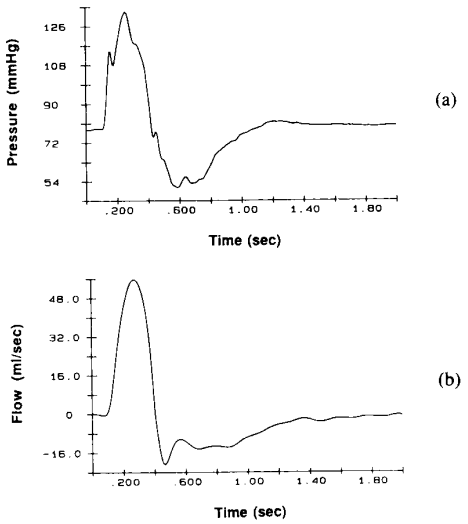

Fig. 6. Sample records of digitized pressure and flow data (from dog 4) sampled at 185 Hz then low-pass filtered with a cutoff of 45 Hz: (a) pressure, (b) flow.

draulic output in and out of the muscle pouch system were available for analysis at any given set of electrical stimulation and hydraulic loading parameters. The electric energy was computed by integrating the current-voltage product with respect to time.

Results

Electrode Characteristics

Fig. 7 shows the voltage rheobase values for the nerve cuff electrode and the intramuscular electrode respectively as a function of time post-implant. The chronaxie values were approximately 50 μs for NCE and 150 μs for IME. Table I shows the average values for both NCE and IME on all subjects at implant day and at termination day. It is clear that the intramuscular electrode requires a higher stimulation voltage to achieve threshold than does the nerve cuff electrode. The IME also has a substantially larger chronaxie value indicating a higher time constant. This is to be expected because of the larger exposed surface area and therefore increased capacitance.

The resistance index computed at a pulse width of 230 μs appears in Fig. 8. The computed impedance started at an initial high value, decreased abruptly to a minimum at one week post-implant then increased again to a stable asymptotic value. Two of the NCE (dogs 2 and 4) showed a very low impedance of 130 Ω compared to 700 Ω for the rest; this is thought to represent either a defect in the construction of the NCE or a parasitic shunt (between the electrode wires and the interstitial fluid) that evolved following the implant. The mean asymptotic IME resistance index was 233 Ω.

To obtain the displaced electrical charge at threshold, the current pulse was integrated with respect to time to yield a waveform similar to the one shown in Fig. 4(c). The displaced charge at threshold appears in Fig. 9(a) and (b) for the NCE and IME. The IME entails on average a

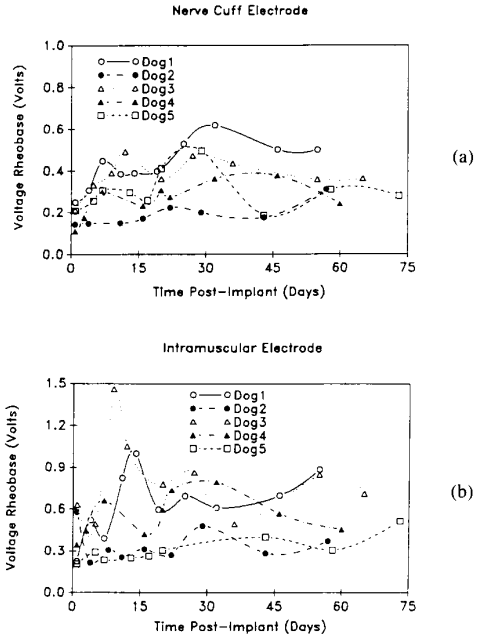

Fig. 7. Computed voltage rheobase by least-squares fit of Lapicque's equation to the strength-duration curve as a function of time following implant for all dogs (1-5): (a) nerve cuff electrode (NCE), (b) intramuscular electrode (IME).

TABLE I
SUMMARY OF THE COMPUTATION OF RHEOBASE AND CHRONAXIE BY LEAST-SQUARES FIT OF LAPICQUE'S EQUATION AT TIME OF IMPLANT AND ONE WEEK BEFORE EVALUATION OF MUSCLE FUNCTION (NCE: NERVE CUFF ELECTRODE; IME: INTRAMUSCULAR ELECTRODE)

Electrode Type & Time	Rheobase (Volts)	Chronaxie (μsec)
NCE (Day 1)	0.18±.06	42±13
NCE (Day 55-60)	0.31±.06	54±14
IME (Day1)	0.40±.20	71±24
IME (Day 55-60)	0.60±.20	185±74

five times greater charge displacement than does the NCE to achieve threshold. Such measures are important to determine the longevity of the battery for a potential stimulator design for the two types of electrodes. These results must be interpreted with care since they were conducted using a single pulse at threshold. To obtain an approximate value of displaced charge for pulse-train stimulation, one would need to multiply the above results by the appropriate number of pulses per train.

Recruitment Properties

The preload was set at 80 mmHg and the afterload at 100 mmHg and the reference output parameters were used. Fig. 10 shows the peak pressure generated inside the muscle pouch as plotted versus the voltage stimulation amplitude for both electrode types (NCE and IME) in dogs 1, 3, and 4. A common feature of all the shown recruitment curves is their sigmoidal shape exhibiting saturation at high levels of stimulation. This recruitment

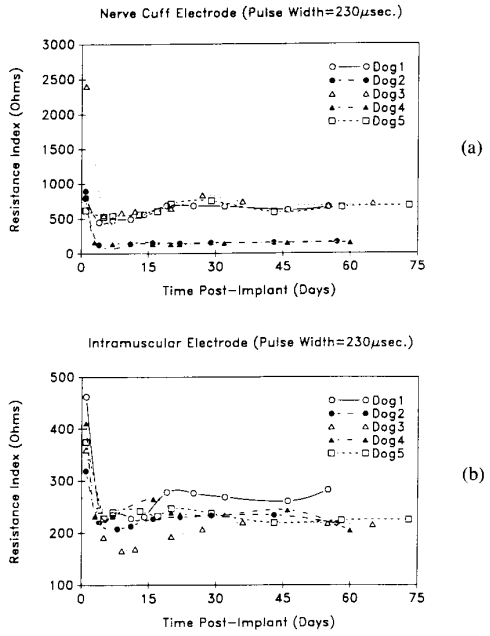

Fig. 8. Computed electrode resistance index (RI) at a pulse width of 230 μs as a function of time following implant for all dogs (1-5): (a) nerve cuff electrode (NCE), (b) intramuscular electrode (IME).

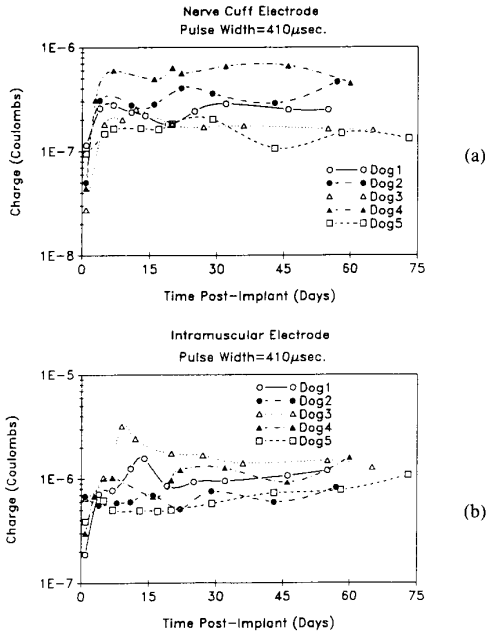

Fig. 9. Displaced electrical charge at threshold voltage stimulus of pulse width 410 μs: (a) nerve cuff electrode (NCE), (b) intramuscular electrode (IME).

curve is characterized by the threshold value below which no significant contraction is produced, a maximum value where saturation first appears, and the slope at the midpoint of the rising portion of the curve. These values then yield a range which is the difference between the stimulation value at the saturation point and the value at threshold.

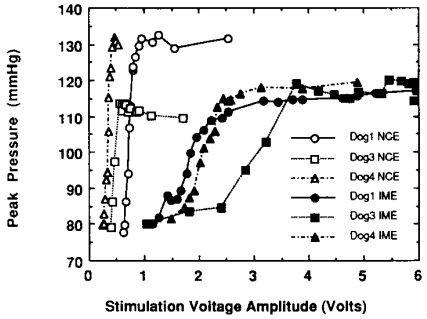

Fig. 10. Recruitment curve of LDM showing peak pressure developed in muscle pouch as a function of stimulation voltage amplitude for dogs 1, 3, and 4. (NCE: nerve cuff electrode, IME: intramuscular electrode). Electrical stimulation parameters are: pulse-train duration of 190 ms, pulse-train frequency of 36 Hz, and pulse width of 230 μs.

In all cases, the NCE had a lower threshold for generating pressure than the IME; this is consistent with the long-term threshold results reported above where the NCE was consistently lower than the IME. Another general feature that surfaces in the comparison of NCE and IME recruitment curves is the steeper slope of pressure generation with respect to stimulation voltage.

All of the IME preparations appear to have threshold voltages between 1 and 1.5 V with similar saturation voltages at approximately 4 V. The NCE preparations, on the other hand, have threshold voltages between 0.25 and 0.65 V (0.65, 0.35, and 0.25 V for dogs 1, 3, and 4, respectively) and saturation voltages ranging between 0.4 and 0.9 V (0.9, 0.5, and 0.4 V for dogs 1, 3, and 4, respectively). Since the absolute values of the various voltages are smaller for NCE than for IME, one can conclude that the IME results provide a smaller relative variability than their NCE counterparts and, therefore offer a higher potential for reproducibility. The range of NCE is 0.3–0.5 V from threshold to saturation while that of IME is approximately 3 V. Nonetheless, although the recruitment curve of NCE is quite sharp, it is not a step-function of an all-or-none characteristic, and as such it does offer the potential for stimulation voltage amplitude modulation of muscle output.

One must keep in mind that the shape of the recruitment curve depends on the frequency and duration of the stimulation pulse train and the pulse-width [16] used.

Electric Energy Requirement

In order to predict the longevity of an implantable device and to compare the energetic efficiencies of the two types of electrodes to achieve similar muscle output the recruitment curve was presented as a function of the electric energy per pulse-train. The results of Fig. 11 show that the NCE require on average 1.5–2 orders of magnitude less electrical stimulation energy than the IME at the onset of saturation on the recruitment curve. The displaced charge required at the same point was also found to be approximately 1 order of magnitude higher for IME than for NCE.

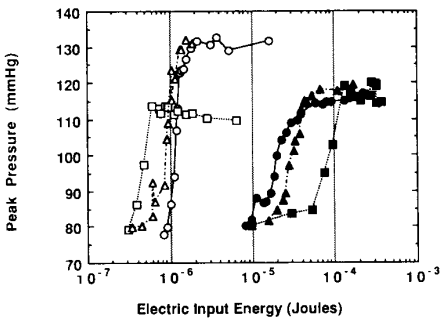

Fig. 11. Recruitment curve of LDM showing peak pressure developed in muscle pouch as a function of electric energy input per pulse-train for dogs 1, 3, and 4. (NCE: nerve cuff electrode, IME: intramuscular electrode). Electrical stimulation parameters are: pulse-train duration of 190 ms, pulse-train frequency of 36 Hz, and pulse width of 230 μs. Legend is same as in Fig. 10.

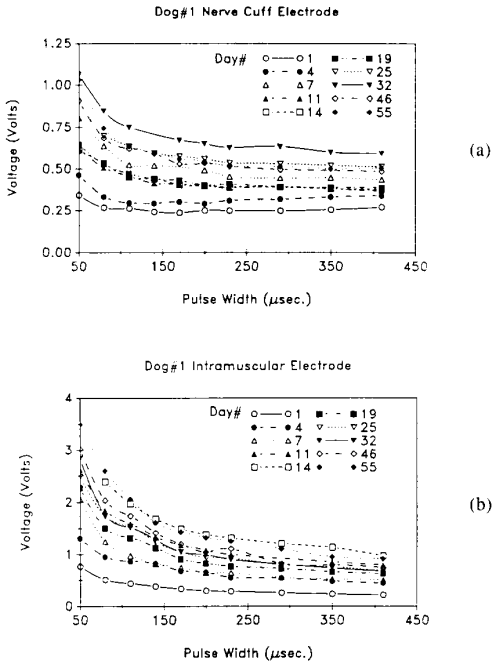

Fig. 12. Dependence of threshold stimulation voltage amplitude on stimulus pulse width (strength-duration curve) at various days following implant for dog 1: (a) nerve cuff electrode (NCE), (b) intramuscular electrode (IME).

Discussion

The visual detection of LDM contraction is a simple but not ideal method of determining threshold. Although it would have been desirable to implant a force-transducer in series with the LDM, such a procedure is not possible at the origin of the muscle because of the width of the latter: the LDM originates from the lower six thoracic processes and indirectly from the thoraco-lumbar fascia and iliac crest. Implanting a transducer at the insertion of the LDM into the humerus would have interfered with, and been complicated by the dog's motion. Although an EMG-based detection methodology could have been adopted, it would have been sensitive to the placement of the measurement electrodes and the varying relationship between EMG magnitude and muscle contraction. Fig. 12 shows that the visual detection is, in fact, sufficient to segregate between the contractions at two adjacent pulse-widths, as attested by the shape of the strength-duration curves considering the random ordering of pulse-widths used in the experiment. Therefore, the large fluctuations in the rheobase shown in Fig. 7 cannot be attributed, except to a small degree, to the use of visual detection in determining thresholds.

The recruitment curve (Fig. 10) showed that the mean peak pressure reached by the NCE was higher than that attained by the IME by approximately 10 mmHg, a significant figure. This difference suggests that the NCE affords a more complete recruitment of the fibers present in the muscle than does the IME, even though the cathode (SP5528) of the IME was purposely placed in close proximity to the TDN branching point.

The sharp recruitment of the NCE can be attractive because it allows to reach maximum contraction with a minimal increase in the stimulation energy, which translates into an improved device longevity; such a steep recruitment curve may not however be desirable because threshold variations and fatigue can shift the recruitment with time [16] so that a fractional increase in the case of NCE might not lead to as predictable a response as an identical change would in the case of IME. Observing the mean size of the fluctuations of the rheobase with time (Fig. 7) indicates a value of 0.2 V for NCE and 0.45 V for IME; 0.2 V represents in the case of NCE approximately the whole range (100 percent) from threshold to onset of saturation, while 0.45 V in the case of IME amounts to less than 15 percent of the corresponding range from threshold to onset of saturation. Although the absolute value of rheobase fluctuations are wider in the case of IME, they are much less important relative to the voltage at saturation than for NCE. This marks a net advantage for the IME in terms of chronic reproducibility of muscle output in the absence of feedback.

Although the recruitment curve of NCE is sharp, modulation of muscle output via stimulation voltage amplitude in the case of NCE is still possible though it might require the use of closed-loop control, whereas a more simple open-loop approach would be satisfactory to a large degree in the case of the IME where the recruitment curve is much more gradual. This advantage of the IME might however be offset by the increased energy requirements of the high stimuli required to achieve maximal contraction.

Type I oxidative fibers usually have smaller nerve fibers with a consequent higher threshold for excitation than type II glycolytic fibers. One would therefore expect the threshold to rise with muscle transformation if the latter entails not only biochemical changes at the level of the contractile proteins but also a decrease in the size of the

associated nerve fibers. Fig. 7 shows a very mild increasing trend with time post-implant and the consequent transformation. This trend is, however, not significant compared to the fluctuations observed from one session to the other, thereby not allowing us to draw any meaningful conclusion. Another complication arises when one considers that the transformation to a type I profile, resulting in a weaker contraction at any given level of recruitment, makes it more difficult to visually detect the contraction of a given number of muscle fibers. Consequently, even if the threshold of a population of fibers were to remain constant throughout their transformation to the weaker type I oxidative fiber, the apparent threshold measured by the visual threshold detection method would be artifactually higher.

Independent of all the electrical characteristics of either electrode, the IME seems to address one of the major shortcomings of the NCE because it avoids direct mechanical contact with the sensitive nerve tissue, thereby reducing the increased danger of nerve injury, death and ensuing inflammation, and fibrosis [15]. This mechanical stability is achieved thanks to the SP5528's being supported by muscle tissue while being positioned close to the nerve branching for effective nondirect nerve stimulation. It must be added that since a controlled-voltage source was used in these results, the use of zero net-area biphasic pulses does not absolutely ensure zero net charge transfer to the tissue as would be the case with a controlled-current source.

It is important to keep in mind that the experimental animals in this study were not deafferented, which implies the possible presence of reflex components in the results presented above. Deafferentiation was not considered because the LDM is supplied by the TDN, from cervical spinal segments C7 and C8, which also innervate other major muscles via the brachial plexus (e.g., triceps, flexors of the hand, pectoralis major). This overlap of innervation does not permit the removal of afferent innervation from the LDM without disrupting the innervation of other muscles whose function is essential for comfortable living in humans.

Conclusion

We can conclude that the nerve cuff electrode offers a lower threshold than the intramuscular electrode, a potential advantage in the total amount of motor units recruited, sharper recruitment characteristics, and an energy consumption at saturation that is nearly two orders of magnitude lower. The nerve cuff electrode appears to be less stable mechanically with two of the five electrodes developing a shunt by a week's time post-implant; it also suffers from relatively larger rheobase fluctuations that equal and sometimes exceed the range of its recruitment curve. The intramuscular electrode avoids the long-standing issue of mechanical friction of the electrode against nerve tissue and is expected to be less injurious than the nerve cuff electrode in long-term applications. The advantages of the IME are, however, achieved dearly in terms of a higher electrical stimulation energy that may be incompatible with a long-term implantable device and a less complete motor unit recruitment than the NCE.

References

[1] M. A. Acker, R. L. Hammond, J. D. Mannion, S. Salmons, and L. W. Stephenson, "An autologous biologic pump motor," *J. Thor. Surg.*, vol. 92, pp. 733-746, 1986.

[2] M. A. Acker, W. A. Anderson, R. L. Hammond, A. J. Chin, J. W. Buchanan, C. C. Morse, A. M. Kelley, and L. W. Stephenson, "Skeletal muscle ventricles in circulation," *Thor. Vasc. Surg.*, vol. 94, pp. 163-174, 1987.

[3] M. A. Acker, J. D. Mannion, and L. W. Stephenson, *Methods of Transforming Skeletal Muscle into a Fatigue-Resistant State: Potential for Cardiac Assistance—Biomechanical Cardiac Assist.*, R. C. J. Chiu, Ed. New York: Futura, 1986.

[4] A. Carpentier and J. D. Chachques, *The Use of Stimulated Skeletal Muscle to Replace Diseased Human Heart Muscle. Biomechanical Cardiac Assist.*, R. C. J. Chiu, Ed. New York: Futura, 1986.

[5] R. C. J. Chiu, I. R. Neilson, A. S. Khalafalla, "The rationale for skeletal muscle-powered counterpulsation devices: An overview," *J. Card. Surg.*, vol. 1-4, pp. 385-392, 1986.

[6] R. C. J. Chiu, G. L. Walsh, M. L. Dewar, *et al.*, "Implantable extra-aortic balloon assist powered by transformed fatigue-resistant skeletal muscle," *J. Thorac. Surg.*, vol. 94, pp. 694-701, 1987.

[7] A. M. Dymond, "Characteristics of the metal-tissue interface of stimulation electrodes," *IEEE Trans. Biomed. Eng.*, vol. 23, pp. 274-280, July 1976.

[8] P. A. Grandjean, K. S. Herpers, I. Bourgeois *et al.*, *Implantable Electronics and Leads for Muscular Cardiac Assistance. Biomechanical Cardiac Assist.*, R. C. J. Chiu, Ed. New York: Futura, 1986.

[9] I. Werner, "The fundamental law of electrostimulation," in *Proc. 2nd Vienna Int. Workshop Functional Electrical Stimulation*, 1986, pp. 1-12.

[10] A. Kantrowitz and W. M. P. McKinnon, "The experimental use of diaphragm as an auxiliary myocardium," *Surg. Forum*, vol. 9, pp. 266, 1959.

[11] A. Kantrowitz, "Functioning autogenous muscle used experimentally as an auxiliary ventricle," *Trans. Am. Soc. Artif. Int. Org.*, vol. 6, p. 305, 1960.

[12] L. Lapicque, "Sur l'excitation électrique des nerfs traitée comme une polarization," *J. Physiol. Pathol. Gener.*, vol. 49, pp. 620-635, 1907.

[13] J. A. Macoviak, L. W. Stephenson, F. Armenti, *et al.*, "Electrical conditioning of in situ skeletal muscle for replacement of myocardium," *J. Surg. Res.*, vol. 32, pp. 429-435, 1982.

[14] G. J. Magovern, F. R. Heckler, P. B. Sang, *et al.*, "Paced latissimus dorsi used for dynamic cardiomyoplasty of left ventricular aneurysms," *Ann. Thorac. Surg.*, vol. 44, pp. 379-388, Oct. 1987.

[15] A. M. Malek, "The characterization of the latissimus dorsi muscle as a power source for use in cardiac assist," M.S. thesis, M.I.T. Dep. Elec. Eng. Comput. Sci., 1988.

[16] J. T. Mortimer, *Motor Prostheses. Handbook of Physiology: the Nervous System, Vol. II, Motor Control*, V. B. Brooks, Ed. Bethesda MD: Amer. Phys. Soc., 1981, pp. 155-187.

[17] I. R. Neilson, S. J. Brister, A. S. Khalafalla, and R. C. J. Chiu, "Left ventricular assistance in dogs using a skeletal muscle powered device for diastolic augmentation," *Heart Transp. IV*, vol. 3, pp. 343-347, 1985.

[18] W. J. Ohley, "Counterpulsation: Theory and Practice," *IEEE Eng. Med. Biol.*, pp. 14-18, Mar. 1986.

[19] S. Salmons and J. Henriksson, "The adaptive response of skeletal muscle to increased use," *Muscle Nerve*, vol. 4, p. 94, 1981.

[20] R. L. Testermann, N. R. Hagfors, and S. L. Schwartz, "Design and evaluation of nerve stimulating electrodes," *Med. Res. Eng.*, vol. 1-2, pp. 6-12, 1971.

[21] G. Walsh, M. Dewar, I. Neilson, *et al.*, "Stimulation parameters of skeletal muscle for cardiac assist," presented at IEEE 8th Annu. Conf. Med. Biol. Soc., 1986.

Adel M. Malek was born in Beirut, Lebanon, in 1965. He received the B.S. and M.S. degrees in electrical engineering and computer science from the Massachusetts Institute of Technology, Cambridge, in 1988 following an internship with Medtronic Inc., Minneapolis, MN.

He is currently enrolled as a first-year student at Harvard Medical School in the M.D.–Ph.D. program of the Harvard-M.I.T. division of Health Sciences and Technology. His research interests include cardiovascular physiology, vascular cell biology, and applications of engineering and control in medicine.

Roger G. Mark (S'59–M'83) was born in Boston, MA, in 1939. He received the Ph.D. degree in electrical engineering from the Massachusetts Institute of Technology, Cambridge, in 1966, and the M.D. degree from Harvard Medical School in 1965.

He is Matsushita Associate Professor of Electrical Engineering in Medicine at MIT, and is currently Co-director of the Harvard-MIT Division of Health Sciences and Technology. He is Co-director of the Arrhythmia Laboratory at Beth Israel Hospital in Boston, and practices internal medicine on a part-time basis. His research interests are biomedical instrumentation, particularly automated cardiac arrhythmia analysis, and cardiovascular physiology.